IEEE Access
Multidisciplinary | Rapid Review | Open Access Journal

Received June 25, 2019, accepted July 19, 2019, date of publication July 31, 2019, date of current version August 15, 2019.

Digital Object Identifier 10.1109/ACCESS.2019.2932147

Average Symbol Error Rate Analysis of QAM Schemes Over Millimeter Wave Fluctuating Two-Ray Fading Channels

MEHMET BILIM [1] **AND NURI KAPUCU** [2]

[1]Department of Electrical and Electronics Engineering, Faculty of Engineering, Nuh Naci Yazgan University, 38170 Kayseri, Turkey

[2]Department of Electrical and Electronics Engineering, Faculty of Engineering, Hitit University, 19030 Corum, Turkey

Corresponding author: Mehmet Bilim (mbilim@nny.edu.tr)

ABSTRACT In this study, analytical expressions are derived by using probability density function approach over millimeter wave fluctuating two-ray (FTR) fading channels for average symbol error rate (ASER) of rectangular quadrature amplitude modulation (RQAM) and cross quadrature amplitude modulation (XQAM) schemes. First, an exact ASER expression for RQAM over millimeter wave FTR fading channels is derived. Second, two different upper bound ASER expressions of RQAM scheme under millimeter wave FTR fading conditions are obtained by using Chernoff and Chiani approximations of Gaussian Q-function. In addition to this, an asymptotic ASER expression for RQAM is also proposed. Then, an analytical formulation is presented for XQAM signaling over millimeter wave FTR fading channels in terms of infinite series representations which rapidly converge. Finally, the numerical results of the proposed analytical expressions are compared with the simulation results in order to validate the analytical findings in this work.

INDEX TERMS Rectangular QAM, Cross QAM, ASER, fluctuating two-ray fading.

I. INTRODUCTION

Quadrature amplitude modulation (QAM) is a bandwidth efficient modulation type and it is used in the field of digital multimedia transmission. The advantages of high power and bandwidth efficiency makes the use of QAM signaling in LTE Advanced and beyond preferable [1]. QAM, is one of many existing modulation techniques, is a promising way of enhancing the spectral efficiency [2]. Besides, QAM schemes are known as useful adaptive modulation schemes, since the constellation size of the QAM signaling can be adjusted depending on the channel quality. QAM methods have drawn considerable research attention due to the fact that it is broadly used in many wireless communication applications such as microwave, high-speed mobile communication systems, and asymmetric subscriber loop, etc [3]–[5]. There are several QAM schemes which are called as rectangular QAM (RQAM), cross QAM (XQAM) and square QAM (SQAM). RQAM is a general modulation technique since it covers a variety of well-known modulations such as SQAM, orthogonal binary frequency-shift keying, quadrature phase-shift keying, binary phase-shift keying [5]. Practically, RQAM has the implementation fields in microwave communications, high rate wireless communications, and telephone-line modems [6], [7]. Among the QAM schemes mentioned above, the optimal QAM signaling is XQAM scheme when the odd number of bits per symbol is transmitted due to its low average symbol energy compared to RQAM [8]. For instance, constellation size between 5-15 bits for XQAMs can be used in asymmetric and high speed subscriber lines [9], [10], while 32-XQAM and 128-XQAM are utilized in digital video broadcasting [11].

Recently, QAM methods have become popular due to its suitability in high speed communications and bandwidth efficiency. The researchers have reported a number of studies on average symbol error rate (ASER) performance of QAM schemes used in different communication systems over different fading channels [12]–[22]. In [12], the ASER of RQAM and XQAM signaling was presented in two-wave with diffuse power (TWDP) fading channels. Closed-form error probability expressions for M-ary XQAM signaling were proposed by using a maximal-ratio combining (MRC) technique in η-μ fading environments in [13]. The authors of [14] analyzed the ASER performance of QAM techniques

The associate editor coordinating the review of this manuscript and approving it for publication was Xiaodong Yang.

in two-way relaying communication networks in the presence of Nakagami-m fading. Dixit and Sahu [15] derived an expression for RQAM technique with selection combining over Nakagami-m fading conditions. The effects of imperfect channel state information on the ASER of hexagonal QAM and RQAM schemes were studied for an amplify-and-forward (AF) protocol under Nakagami-m fading conditions [16]. The impact of the channel estimation [23], [24] is important for the realization of the practical scenarios. In another study [17], the authors performed an analytical evaluation on the performance of QAM methods used in multiple AF relaying system over Rayleigh fading channels. In [18], a simple approximation was developed for general-order RQAM with MRC receiver in Nakagami-m environments. In addition, hexagonal QAM and RQAM schemes were used in an orthogonal frequency division multiplexing with 3-hop AF relaying system and the authors presented the performance results over mixed Rician/Rayleigh fading links [19]. In [20], error probability of XQAM method was derived over Nakagami-m, Hoyt, Rice, and Rayleigh conditions by performing MRC at the receiver. Khan *et al.* [21] proposed two algorithms called rectangular contour algorithm (RCA) and improved RCA for blind equalization techniques of RQAM signaling with odd bit. In [22], a comprehensive study for QAM analysis over κ-μ shadowed fading channels is presented.

The studies mentioned above have focused on the performance analysis of QAM signaling over well-known fading conditions such as Rice, Rayleigh, Hoyt, Nakagami-m, and shadowed etc. As far as we know, there is no work that analyses and presents the ASER performance of RQAM and XQAM techniques over millimeter wave (mmWave) fluctuating two-ray (FTR) fading channels. FTR fading distribution has been recently presented as a channel model which well captures the effects of wireless medium in mmWave and device-to-device environments [25], [26]. Very recently, an outdoor measurement at 28 GHz explored that the well-known small-scale fading distributions such as Rician, Nakagami-m and Rayleigh cannot accurately reflect the random fluctuations in millimeter wave signals [27]. In order to overcome this, the FTR fading is proposed which is more accurate compared to Rayleigh, Nakagami-m, Rician models and to the best of our knowledge, there are only a few works over this new fading channel which can be found in [28]–[30]. Although the FTR fading distribution contains classical unimodal fading models such as Rician or Rayleigh special cases, this model is inherently bimodal. At the same time, the mmWave FTR model is a great and appropriate fading model which takes the large heterogeneity of random fluctuations into consideration that effect the mmWave radio signal when propagating in the presence of multiple scatters. Also, this model is a native generalization of the TWDP fading model that allows the fixed amplitude specular waves associated with line-of-sight propagation to randomly fluctuate. In addition to these advantages, it also contains some conventional fading distributions as special cases, i.e., Rayleigh, Rician, Rician shadowed, one-sided Gaussian, Nakagami-q (Hoyt), Nakagami-m, and TWDP. The mmWave FTR fading model turns into these particular cases by using the parameter definitions [25], [26].

Motivated by the suitability of FTR fading for millimeter wave communications and bandwidth efficient high speed transmission capability of QAM signaling, we derive new and novel analytical expressions for RQAM and XQAM schemes over millimeter wave FTR fading channels for the first time in the literature in this work. First, we derive the exact expression for ASER of RQAM system over millimeter wave FTR fading channels in terms of bivariate Meijer's G function and then, we propose two different upper bounds for the ASER of RQAM based on well-known approximations of Gaussian Q-function. Second, we also obtain an asymptotic ASER expression of RQAM system to illustrate the behaviors of the considered system at the high signal to noise ratio (SNR) regime. Then, we evaluate the performance of XQAM scheme over FTR fading channels. Finally, the obtained analytical results are compared to the corresponding simulations for validation purpose.

II. SYSTEM AND CHANNEL MODELS

Consider a single-input single-output (SISO) wireless network over FTR fading channels and let γ denote the instantaneous SNR. $\overline{\gamma} = (E_b/N_0)\,2\sigma^2(1+K)$ is the average SNR [28]. E_b is the energy per bit, N_0 is the additive white Gaussian noise (AWGN) and σ^2 is the variance of Gaussian noise. The probability density function (PDF) of instantaneous SNR, $f_\gamma(\gamma)$, can be given as [28]

$$f_\gamma(\gamma) = v\sum_{j=0}^{\infty} A_j\gamma^j \exp\left(-\frac{\gamma}{2\sigma^2}\right) \tag{1}$$

where $v = \frac{m^m}{\Gamma(m)}$, $A_j = \frac{K^j d_j}{j!\Gamma(j+1)(2\sigma^2)^{j+1}}$ and

$$d_j = \sum_{k=0}^{\infty}\binom{j}{k}\left(\frac{\Delta}{2}\right)^k\sum_{l=0}^{k}\binom{k}{l}\Gamma(j+m+2l-k) \times \exp\left(\frac{\pi(2l-k)i}{2}\right)\times\left((m+K)^2-(K\Delta)^2\right)^{-\frac{(j+m)}{2}} \times P_{j+m-1}^{k-2l}\left(\frac{m+K}{\sqrt{(m+K)^2-(K\Delta)^2}}\right) \tag{2}$$

where $\Gamma(\cdot)$ is the Gamma function, m is a Nakagami-m random variable, K is the ratio of the average power of the dominant waves to the average power of the remaining diffuse multipath and it is defined by $K = \frac{V_1^2+V_2^2}{2\sigma^2}$. Δ denotes the relation between the powers of two dominant waves and given by $\Delta = \frac{2V_1V_2}{V_1^2+V_2^2}$. V_1 and V_2 are two specular components, $P_b^a(\cdot)$ is the Legendre functions of the first kind [31, eq. (8.702)]. j and l are the indexes of the summations in eqs (1) and (2). The FTR fading model includes several well-known fading models for different values of m, K and Δ such as

Rayleigh, Nakagami-q, Rician, Rician shadowed and the one-sided Gaussian as mentioned before.

III. PERFORMANCE ANALYSIS

In this section, we provide an exact and two different approximate derivations of ASER for RQAM and an ASER expression for XQAM of the considered system under FTR fading conditions.

A. EXACT ASER ANALYSIS FOR RQAM

The ASER, Pe, is generally defined as [5]

$$Pe = \int_0^\infty p(e|\gamma) f_\gamma(\gamma)\, d\gamma \tag{3}$$

where $p(e|\gamma)$ is the conditional error probability for AWGN and it is given for M-ary RQAM as [32]

$$p(e|\gamma) = 2pQ\left(a\sqrt{\gamma}\right) + 2qQ\left(b\sqrt{\gamma}\right) - 4pqQ\left(a\sqrt{\gamma}\right)Q\left(b\sqrt{\gamma}\right) \tag{4}$$

where $Q(\cdot)$ is the Gaussian Q-function. $M = M_I \times M_Q$, $p = 1 - (1/M_I)$, $q = 1 - \left(1/M_Q\right)$, $b = \beta a$, $\beta = d_Q/d_I$, $a = \sqrt{6/\left(M_I^2 - 1\right) + \left(M_Q^2 - 1\right)\beta^2}$, d_Q and d_I are the quadrature and in-phase decision distance, respectively.

Substituting (1) and (4) into (3), we have

$$Pe = \int_0^\infty \left\{2pQ\left(a\sqrt{\gamma}\right) + 2qQ\left(b\sqrt{\gamma}\right) - 4pqQ\left(a\sqrt{\gamma}\right)Q\left(b\sqrt{\gamma}\right)\right\} \times v\sum_{j=0}^\infty A_j\gamma^j \exp\left(-\frac{\gamma}{2\sigma^2}\right)d\gamma \tag{5}$$

After some manipulations and using $Q(x) = (1/2)\,erfc\left(x/\sqrt{2}\right)$, the expression in (5) can be rewritten as follows

$$Pe = \int_0^\infty \left\{p\,\mathrm{erfc}\left(a\sqrt{\frac{\gamma}{2}}\right) + q\,\mathrm{erfc}\left(b\sqrt{\frac{\gamma}{2}}\right) - pq\mathrm{erfc}\left(a\sqrt{\frac{\gamma}{2}}\right) \times \mathrm{erfc}\left(b\sqrt{\frac{\gamma}{2}}\right)\right\} v\sum_{j=0}^\infty A_j\gamma^j \exp\left(-\frac{\gamma}{2\sigma^2}\right)d\gamma \tag{6}$$

where erfc $(\cdot)$ is the complementary error function. By using [33, eq. (8.4.14.2)], 6 becomes as shown in (7) at the top of next page.

where G $(\cdot|\cdot)$ is the Meijer's G function [31]. Then, F_1 and F_2 are derived with the aid of [33, eq. (2.24.3.1)] as

$$F_1 = \left(\frac{1}{2\sigma^2}\right)^{-(j+1)} \mathrm{G}_{2,2}^{2,1}\left(a^2\sigma^2 \middle| \begin{matrix}\Delta(1,-j), \Delta(1,1)\\ \Delta(1,0.5)\end{matrix}\right)$$
$$F_2 = \left(\frac{1}{2\sigma^2}\right)^{-(j+1)} \mathrm{G}_{2,2}^{2,1}\left(b^2\sigma^2 \middle| \begin{matrix}\Delta(1,-j), \Delta(1,1)\\ \Delta(1,0.5)\end{matrix}\right) \tag{8}$$

where $\Delta(u,t) = \frac{t}{u}, \frac{t+1}{u}, \ldots, \frac{t+u-1}{u}$. In order to obtain a solution for F_3, we use the identity between exponential function and Meijer's G function in [33, eq. (8.4.3.1)] and we get

$$F_3 = \frac{pq}{\pi}\int_0^\infty G_{1,2}^{2,0}\left(\frac{a^2\gamma}{2} \middle| \begin{matrix}1\\ 0, 0.5\end{matrix}\right) G_{1,2}^{2,0}\left(\frac{b^2\gamma}{2} \middle| \begin{matrix}1\\ 0, 0.5\end{matrix}\right) \times G_{0,1}^{1,0}\left(\frac{\gamma}{2\sigma^2} \middle| \begin{matrix}-\\ 0\end{matrix}\right)\gamma^j d\gamma \tag{9}$$

With the help of [34, eq. (07.34.21.0081.01)], F_3 is derived as

$$F_3 = \left(\frac{a^2}{2}\right)^{-(j+1)} \times \mathrm{G}_{2,1:1,2:0,1}^{0,2:2,0:1,0}\left(\begin{matrix}-j, -j-0.5\\ -j-1\end{matrix} \middle| \begin{matrix}1\\ 0, 0.5\end{matrix} \middle| \begin{matrix}-\\ 0\end{matrix} \middle| \frac{b^2}{a^2}, \frac{1}{\sigma^2 a^2}\right) \tag{10}$$

where $G_{p,q:p_1,q_1:p_2,q_2}^{m,n:m_1,n_1:m_2,n_2}[\cdot|\cdot|\cdot|\cdot,\cdot]$ is the bivariate Meijer's G function. The exact ASER expression for RQAM is obtained by inserting (8) and (10) into (7), as shown at the top of the next page, and it is given below

$$\begin{aligned}Pe = v\sum_{j=0}^\infty A_j\Bigg[&\left(\frac{1}{2\sigma^2}\right)^{-(j+1)} \times \mathrm{G}_{2,2}^{2,1}\left(a^2\sigma^2 \middle| \begin{matrix}\Delta(1,-j), \Delta(1,1)\\ \Delta(1,0.5)\end{matrix}\right) + \left(\frac{1}{2\sigma^2}\right)^{-(j+1)} \\ &\times \mathrm{G}_{2,2}^{2,1}\left(b^2\sigma^2 \middle| \begin{matrix}\Delta(1,-j), \Delta(1,1)\\ \Delta(1,0.5)\end{matrix}\right) - \left(\frac{a^2}{2}\right)^{-(j+1)} \\ &\times \mathrm{G}_{2,1:1,2:0,1}^{0,2:2,0:1,0}\left(\begin{matrix}-j, -j-0.5\\ -j-1\end{matrix} \middle| \begin{matrix}1\\ 0, 0.5\end{matrix} \middle| \begin{matrix}-\\ 0\end{matrix} \middle| \frac{b^2}{a^2}, \frac{1}{\sigma^2 a^2}\right)\Bigg]\end{aligned} \tag{11}$$

Even though (11) is an exact ASER expression for RQAM schemes over mmWave FTR fading channels, this expression is very difficult to compute in common software packages since the bivariate Meijer's G function is not built-in function in Matlab, Mathematica, and Maple. In what follows, two different approximations for the ASER of RQAM in simple and easy-to-compute form will be derived.

B. ASER ANALYSIS WITH CHERNOFF APPROXIMATION FOR RQAM

To facilitate the analysis, we require to use an approximation for $Q(\cdot)$ functions in (4). The Chernoff approximation is a well-known approximation of $Q(\cdot)$ and it is given by $Q(z) \approx \frac{1}{2}e^{-z^2/2}$ [35]. By using the Chernoff approximation, $p(e|\gamma)$ in (4) is rewritten as

$$p(e|\gamma) \approx p\left[e^{-\frac{a^2}{2}\gamma}\right] + q\left[e^{-\frac{b^2}{2}\gamma}\right] - pq\left[e^{-\frac{a^2+b^2}{2}\gamma}\right] \tag{12}$$

$$Pe = v\sum_{j=0}^{\infty}A_j\Bigg[\underbrace{\frac{p}{\sqrt{\pi}}\int_0^{\infty}G_{1,2}^{2,0}\left(\frac{a^2\gamma}{2}\middle|\begin{matrix}1\\0,0.5\end{matrix}\right)\gamma^j\exp\left(-\frac{\gamma}{2\sigma^2}\right)d\gamma}_{F_1} + \underbrace{\frac{q}{\sqrt{\pi}}\int_0^{\infty}G_{1,2}^{2,0}\left(\frac{b^2\gamma}{2}\middle|\begin{matrix}1\\0,0.5\end{matrix}\right)\gamma^j\exp\left(-\frac{\gamma}{2\sigma^2}\right)d\gamma}_{F_2} - \underbrace{\frac{pq}{\pi}\int_0^{\infty}G_{1,2}^{2,0}\left(\frac{a^2\gamma}{2}\middle|\begin{matrix}1\\0,0.5\end{matrix}\right)G_{1,2}^{2,0}\left(\frac{b^2\gamma}{2}\middle|\begin{matrix}1\\0,0.5\end{matrix}\right)\gamma^j\exp\left(-\frac{\gamma}{2\sigma^2}\right)d\gamma}_{F_3}\Bigg] \quad (7)$$

Substituting (1) and (12) into (3), the ASER formulation with Chernoff approximation for RQAM becomes

$$Pe_{Chernoff} = \int_0^{\infty}\left\{p\left[e^{-\frac{a^2}{2}\gamma}\right]+q\left[e^{-\frac{b^2}{2}\gamma}\right]-pq\left[e^{-\frac{a^2+b^2}{2}\gamma}\right]\right\} \times v\sum_{j=0}^{\infty}A_j\gamma^j\exp\left(-\frac{\gamma}{2\sigma^2}\right)d\gamma \quad (13)$$

Since the $Pe_{Chernoff}$ expression in (13) has three similar integrals, after some mathematical manipulations and using [31, eq. (3.381.4)], we derive the ASER as follows

$$\begin{aligned}Pe_{Chernoff} = {} & pv\sum_{j=0}^{\infty}A_j\left(\frac{a^2}{2}+\frac{1}{2\sigma^2}\right)^{-(j+1)}\Gamma(j+1)\\ & + qv\sum_{j=0}^{\infty}A_j\left(\frac{b^2}{2}+\frac{1}{2\sigma^2}\right)^{-(j+1)}\Gamma(j+1)\\ & - pqv\sum_{j=0}^{\infty}A_j\left(\frac{a^2}{2}+\frac{b^2}{2}+\frac{1}{2\sigma^2}\right)^{-(j+1)}\Gamma(j+1)\end{aligned} \quad (14)$$

C. ASER ANALYSIS WITH CHIANI APPROXIMATION FOR RQAM

To analyze the ASER for RQAM with a different way, we use the Chiani approximation of Gaussian Q-function which is expressed by $Q(z) \approx \frac{1}{12}e^{-z^2/2}+\frac{1}{4}e^{-2z^2/3}$ [36]. By using the Chiani approximation, $p(e|\gamma)$ in (4) is rewritten as

$$\begin{aligned}p(e|\gamma) \approx {} & 2p\left[\frac{1}{12}e^{-\frac{a^2}{2}\gamma}+\frac{1}{4}e^{-\frac{2a^2}{3}\gamma}\right]\\ & + 2q\left[\frac{1}{12}e^{-\frac{b^2}{2}\gamma}+\frac{1}{4}e^{-\frac{2b^2}{3}\gamma}\right]\\ & - 4pq\left[\frac{1}{144}e^{-\left(\frac{a^2+b^2}{2}\right)\gamma}+\frac{1}{48}e^{-\left(\frac{a^2}{2}+\frac{2b^2}{3}\right)\gamma}\right.\\ & \left.+\frac{1}{48}e^{-\left(\frac{2a^2}{3}+\frac{b^2}{2}\right)\gamma}+\frac{1}{16}e^{-\left(\frac{2a^2+2b^2}{3}\right)\gamma}\right]\end{aligned} \quad (15)$$

By inserting (15) and (1) into (3), we have

$$Pe_{Chiani} = v\sum_{j=0}^{\infty}A_j\left[Q_1+Q_2-Q_3\right] \quad (16)$$

where

$$Q_1 = 2p\int_0^{\infty}\left[\frac{1}{12}e^{-\frac{a^2}{2}\gamma}+\frac{1}{4}e^{-\frac{2a^2}{3}\gamma}\right]\gamma^j\exp\left(-\frac{\gamma}{2\sigma^2}\right)d\gamma \quad (17)$$

$$Q_2 = 2q\int_0^{\infty}\left[\frac{1}{12}e^{-\frac{b^2}{2}\gamma}+\frac{1}{4}e^{-\frac{2b^2}{3}\gamma}\right]\gamma^j\exp\left(-\frac{\gamma}{2\sigma^2}\right)d\gamma \quad (18)$$

$$\begin{aligned}Q_3 = {} & 4pq\int_0^{\infty}\left[\frac{1}{144}e^{-\left(\frac{a^2+b^2}{2}\right)\gamma}+\frac{1}{48}e^{-\left(\frac{a^2}{2}+\frac{2b^2}{3}\right)\gamma}\right.\\ & \left.+\frac{1}{48}e^{-\left(\frac{2a^2}{3}+\frac{b^2}{2}\right)\gamma}+\frac{1}{16}e^{-\left(\frac{2a^2+2b^2}{3}\right)\gamma}\right]\\ & \times\gamma^j\exp\left(-\frac{\gamma}{2\sigma^2}\right)d\gamma\end{aligned} \quad (19)$$

Now, we have eight similar integrals in Q_1, Q_2 and Q_3 to be solved for deriving an ASER expression with Chiani approximation for RQAM over FTR fading channels. To proceed, with the use of [31, eq. (3.381.4)] and after performing some analytical manipulations, we get

$$\begin{aligned}Q_1 = {} & 2p\left(\frac{1}{12}\left(\frac{a^2}{2}+\frac{1}{2\sigma^2}\right)^{-(j+1)}\Gamma(j+1)\right.\\ & \left.+\frac{1}{4}\left(\frac{2a^2}{3}+\frac{1}{2\sigma^2}\right)^{-(j+1)}\Gamma(j+1)\right)\end{aligned} \quad (20)$$

$$Q_2 = 2q\left(\frac{1}{12}\left(\frac{b^2}{2}+\frac{1}{2\sigma^2}\right)^{-(j+1)}\Gamma(j+1)\right.$$

$$+\frac{1}{4}\left(\frac{2b^2}{3}+\frac{1}{2\sigma^2}\right)^{-(j+1)}\Gamma(j+1)\Bigg) \tag{21}$$

$$\begin{aligned}Q_3 = 4pq\Bigg(&\frac{1}{144}\left(\frac{a^2+b^2}{2}+\frac{1}{2\sigma^2}\right)^{-(j+1)}\Gamma(j+1)\\&+\frac{1}{48}\left(\frac{a^2}{2}+\frac{2b^2}{3}+\frac{1}{2\sigma^2}\right)^{-(j+1)}\Gamma(j+1)\\&+\frac{1}{48}\left(\frac{2a^2}{3}+\frac{b^2}{2}+\frac{1}{2\sigma^2}\right)^{-(j+1)}\Gamma(j+1)\\&+\frac{1}{16}\left(\frac{2a^2+2b^2}{3}+\frac{1}{2\sigma^2}\right)^{-(j+1)}\Gamma(j+1)\Bigg)\end{aligned} \tag{22}$$

After putting Q_1, Q_2 and Q_3 in (16), an ASER expression with Chiani approximation for RQAM of the considered system in the presence of FTR fading is derived as follows

$$\begin{aligned}Pe_{Chiani} = v\sum_{j=0}^{\infty}\frac{K^j d_j}{j!\,(2\sigma^2)^{j+1}}&\times\Bigg[\Bigg\{2p\left(\frac{1}{12}\left(\frac{a^2}{2}+\frac{1}{2\sigma^2}\right)^{-(j+1)}+\frac{1}{4}\left(\frac{2a^2}{3}+\frac{1}{2\sigma^2}\right)^{-(j+1)}\right)\Bigg\}\\&+\Bigg\{2q\left(\frac{1}{12}\left(\frac{b^2}{2}+\frac{1}{2\sigma^2}\right)^{-(j+1)}+\frac{1}{4}\left(\frac{2b^2}{3}+\frac{1}{2\sigma^2}\right)^{-(j+1)}\right)\Bigg\}\\&-\Bigg\{4pq\Bigg(\frac{1}{144}\left(\frac{a^2+b^2}{2}+\frac{1}{2\sigma^2}\right)^{-(j+1)}\\&+\frac{1}{48}\left(\frac{a^2}{2}+\frac{2b^2}{3}+\frac{1}{2\sigma^2}\right)^{-(j+1)}\\&+\frac{1}{48}\left(\frac{2a^2}{3}+\frac{b^2}{2}+\frac{1}{2\sigma^2}\right)^{-(j+1)}\\&+\frac{1}{16}\left(\frac{2a^2+2b^2}{3}+\frac{1}{2\sigma^2}\right)^{-(j+1)}\Bigg)\Bigg\}\Bigg]\end{aligned} \tag{23}$$

So far as we know that the expressions, Pe_{Chiani} in (23) and $Pe_{Chernoff}$ in (14), are presented for the first time in the literature. Now, we investigate the asymptotic behavior of the ASER at high SNR to specify the diversity order acquired by the considered system when Chiani approximation is used. With the assumption of $\overline{\gamma}\to\infty$, the $2\sigma^2$ approaches to ∞ and truncating the infinite summation at $j=0$, the expression in (23) is simplified and obtained in asymptotic form as

$$\begin{aligned}Pe_{Chiani}^{\infty} &= v\frac{d_0}{2\sigma^2}\times\Bigg[\Bigg\{2p\left(\frac{1}{12}\left(\frac{a^2}{2}\right)^{-1}+\frac{1}{4}\left(\frac{2a^2}{3}\right)^{-1}\right)\Bigg\}\\&+\Bigg\{2q\left(\frac{1}{12}\left(\frac{b^2}{2}\right)^{-1}+\frac{1}{4}\left(\frac{2b^2}{3}\right)^{-1}\right)\Bigg\}\\&-\Bigg\{4pq\Bigg(\frac{1}{144}\left(\frac{a^2+b^2}{2}\right)^{-1}+\frac{1}{48}\left(\frac{a^2}{2}+\frac{2b^2}{3}\right)^{-1}\\&+\frac{1}{48}\left(\frac{2a^2}{3}+\frac{b^2}{2}\right)^{-1}+\frac{1}{16}\left(\frac{2a^2+2b^2}{3}\right)^{-1}\Bigg)\Bigg\}\Bigg]\end{aligned} \tag{24}$$

D. EXACT ASER ANALYSIS FOR XQAM

For XQAM, $p(e|\gamma)$ is given as [13]

$$\begin{aligned}p(e|\gamma) &= g_1 Q_z\left(a_0\sqrt{\gamma},\pi/2\right)+\frac{4}{M}Q_z\left(a_1\sqrt{\gamma},\pi/2\right)\\&-g_2 Q_z\left(a_0\sqrt{\gamma},\pi/4\right)-\frac{8}{M}\sum_{k=1}^{w-1}Q_z\left(a_0\sqrt{\gamma},\alpha_k\right)\\&-\frac{4}{M}\sum_{k=1}^{w-1}Q_z\left(a_k\sqrt{\gamma},\beta_k^{+}\right)+\frac{4}{M}\sum_{k=2}^{w}Q_z\left(a_k\sqrt{\gamma},\beta_k^{-}\right)\end{aligned} \tag{25}$$

where $M=2^5, 2^7, \ldots$, $w=\frac{\sqrt{2M}}{8}$, $a_0=\sqrt{\frac{96}{(31M-32)}}$, $a_k=\sqrt{2}\,ka_0$, $k=1,2,3,\ldots,w$, $g_2=4-\frac{12}{\sqrt{2M}}+\frac{12}{2M}$, $g_1=4-\frac{6}{\sqrt{2M}}$, $\alpha_k=\arctan\left(\frac{1}{2k+1}\right)$, $k=1,2,\ldots,(w-1)$, $\beta_k^{-}=\arctan\left(\frac{k}{k-1}\right)$, $k=2,3\ldots,w$, $\beta_k^{+}=\arctan\left(\frac{k}{k+1}\right)$ and, $k=1,2,\ldots,(w-1)$. $Q_z(\cdot,\cdot)$ is the generalized Marcum Q-function. Substituting (25) and (1) into (3), we have

$$\begin{aligned}Pe_{XQAM} &= v\sum_{j=0}^{\infty}A_j\Bigg[\underbrace{\int_0^{\infty}g_1 Q_z\left(a_0\sqrt{\gamma},\pi/2\right)\gamma^j\exp\left(-\frac{\gamma}{2\sigma^2}\right)d\gamma}_{D_1}\\&+\underbrace{\int_0^{\infty}\frac{4}{M}Q_z\left(a_1\sqrt{\gamma},\pi/2\right)\gamma^j\exp\left(-\frac{\gamma}{2\sigma^2}\right)d\gamma}_{D_2}\\&-\underbrace{\int_0^{\infty}g_2 Q_z\left(a_0\sqrt{\gamma},\pi/4\right)\gamma^j\exp\left(-\frac{\gamma}{2\sigma^2}\right)d\gamma}_{D_3}\end{aligned}$$

$$- \underbrace{\int_0^\infty \frac{8}{M} \sum_{k=1}^{w-1} Q_z\left(a_0\sqrt{\gamma}, \alpha_k\right)\gamma^j \exp\left(-\frac{\gamma}{2\sigma^2}\right) d\gamma}_{D_4}$$
$$- \underbrace{\int_0^\infty \frac{4}{M} \sum_{k=1}^{w-1} Q_z\left(a_k\sqrt{\gamma}, \beta_k^+\right)\gamma^j \exp\left(-\frac{\gamma}{2\sigma^2}\right) d\gamma}_{D_5}$$
$$\left. + \underbrace{\int_0^\infty \frac{4}{M} \sum_{k=2}^{w} Q_z\left(a_k\sqrt{\gamma}, \beta_k^-\right)\gamma^j \exp\left(-\frac{\gamma}{2\sigma^2}\right) d\gamma}_{D_6} \right] \tag{26}$$

The expression in (26) contains six similar integrals such as D_1-D_6. In order to solve D_1, D_1 is re-arranged with the use of the infinite series representation of generalized Marcum Q-function [37, eq. (4.37)] as follows

$$\begin{aligned} D_1 &= \int_0^\infty g_1 Q_z\left(a_0\sqrt{\gamma}, \pi/2\right)\gamma^j \exp\left(-\frac{\gamma}{2\sigma^2}\right) d\gamma \\ &= g_1 \exp\left(-\frac{(\pi/2)^2}{2}\right) \sum_{r=1-z}^{\infty} \left(\frac{a_0}{(\pi/2)}\right)^r \\ &\quad \times \int_0^\infty \exp\left(-\frac{(a_0)^2\gamma}{2} - \frac{\gamma}{2\sigma^2}\right)\gamma^{r+j} I_r\left(\frac{a_0\pi}{2}\sqrt{\gamma}\right) d\gamma \end{aligned} \tag{27}$$

where $I_r(\cdot)$ is the modified Bessel function. To proceed, we need to use the series representation of $I_r(\cdot)$ which is defined by $I_r(x) = \left((1/2)x\right)^r \sum_{h=0}^{\infty} \frac{\left((1/4)x^2\right)^h}{h!\Gamma(r+h+1)}$ [38, eq. (9.6.10)]. Hence, D_1 becomes

$$\begin{aligned} D_1 &= g_1 \exp\left(-\frac{(\pi/2)^2}{2}\right) \sum_{r=1-z}^{\infty} \left(\frac{a_0}{(\pi/2)}\right)^r \left(\frac{a_0\pi}{4}\right)^r \\ &\quad \times \sum_{h=0}^{\infty} \left(\frac{\left(\frac{a_0\pi}{2}\right)^2 \frac{1}{4}}{h!\Gamma(r+h+1)}\right)^h \\ &\quad \times \int_0^\infty \exp\left(-\frac{(a_0)^2\gamma}{2} - \frac{\gamma}{2\sigma^2}\right)\gamma^{r+j+h} d\gamma \end{aligned} \tag{28}$$

By using [31, eq. (3.381.4)], D_1 is derived as

$$\begin{aligned} D_1 &= g_1 \exp\left(-\frac{(\pi/2)^2}{2}\right) \sum_{r=1-z}^{\infty} \left(\frac{a_0}{(\pi/2)}\right)^r \left(\frac{a_0\pi}{4}\right)^r \\ &\quad \times \sum_{h=0}^{\infty} \left(\frac{\left(\frac{a_0\pi}{2}\right)^2 \frac{1}{4}}{h!\Gamma(r+h+1)}\right)^h \\ &\quad \times \left(\frac{(a_0)^2}{2} + \frac{1}{2\sigma^2}\right)^{-(r+j+h+1)} \Gamma(r+j+h+1) \end{aligned} \tag{29}$$

Then, D_2-D_6 are obtained by following the same analytical steps used for D_1 as

$$\begin{aligned} D_2 &= \frac{4}{M} \exp\left(-\frac{(\pi/2)^2}{2}\right) \sum_{r=1-z}^{\infty} \left(\frac{(a_1)^2}{2}\right)^r \\ &\quad \times \sum_{h=0}^{\infty} \left(\frac{\left(\frac{a_1\pi}{2}\right)^2 \frac{1}{4}}{h!\Gamma(r+h+1)}\right)^h \\ &\quad \times \left(\frac{(a_1)^2}{2} + \frac{1}{2\sigma^2}\right)^{-(r+j+h+1)} \Gamma(r+j+h+1) \end{aligned} \tag{30}$$

$$\begin{aligned} D_3 &= g_2 \exp\left(-\frac{(\pi/4)^2}{2}\right) \sum_{r=1-z}^{\infty} \left(\frac{(a_0)^2}{2}\right)^r \\ &\quad \times \sum_{h=0}^{\infty} \left(\frac{\left(\frac{a_0\pi}{2}\right)^2 \frac{1}{4}}{h!\Gamma(r+h+1)}\right)^h \\ &\quad \times \left(\frac{(a_0)^2}{2} + \frac{1}{2\sigma^2}\right)^{-(r+j+h+1)} \Gamma(r+j+h+1) \end{aligned} \tag{31}$$

$$\begin{aligned} D_4 &= \frac{8}{M} \sum_{k=1}^{w-1} \exp\left(-\frac{(\alpha_k)^2}{2}\right) \sum_{r=1-z}^{\infty} \left(\frac{a_0}{\alpha_k}\right)^r \left(\frac{a_0\alpha_k}{2}\right)^r \\ &\quad \times \sum_{h=0}^{\infty} \left(\frac{(a_0\alpha_k)^2 \frac{1}{4}}{h!\Gamma(r+h+1)}\right)^h \\ &\quad \times \left(\frac{(a_0)^2}{2} + \frac{1}{2\sigma^2}\right)^{-(r+j+h+1)} \Gamma(r+j+h+1) \end{aligned} \tag{32}$$

$$\begin{aligned} D_5 &= \frac{4}{M} \sum_{k=1}^{w-1} \exp\left(-\frac{(\beta_k^+)^2}{2}\right) \sum_{r=1-z}^{\infty} \left(\frac{a_k}{\beta_k^+}\right)^r \left(\frac{a_k\beta_k^+}{2}\right)^r \\ &\quad \times \sum_{h=0}^{\infty} \left(\frac{(a_k\beta_k^+)^2 \frac{1}{4}}{h!\Gamma(r+h+1)}\right)^h \\ &\quad \times \left(\frac{(a_k)^2}{2} + \frac{1}{2\sigma^2}\right)^{-(r+j+h+1)} \Gamma(r+j+h+1) \end{aligned} \tag{33}$$

$$\begin{aligned} D_6 &= \frac{4}{M} \sum_{k=2}^{w} \exp\left(-\frac{(\beta_k^-)^2}{2}\right) \sum_{r=1-z}^{\infty} \left(\frac{a_k}{\beta_k^-}\right)^r \left(\frac{a_k\beta_k^-}{2}\right)^r \\ &\quad \times \sum_{h=0}^{\infty} \left(\frac{(a_k\beta_k^-)^2 \frac{1}{4}}{h!\Gamma(r+h+1)}\right)^h \\ &\quad \times \left(\frac{(a_k)^2}{2} + \frac{1}{2\sigma^2}\right)^{-(r+j+h+1)} \Gamma(r+j+h+1) \end{aligned} \tag{34}$$

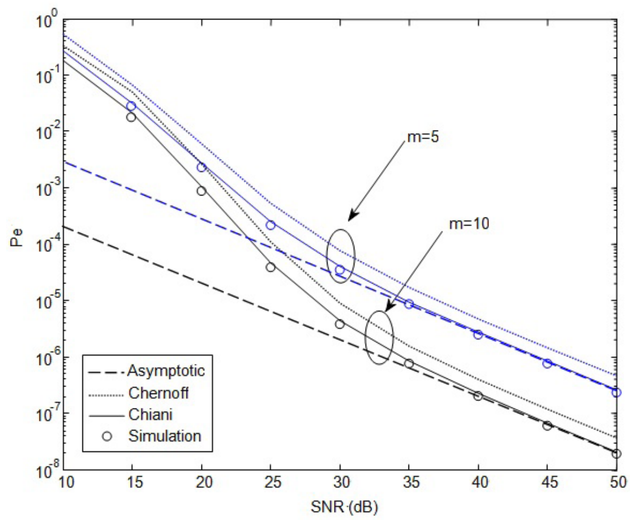

FIGURE 1. ASER performance of 4 × 2 RQAM with $K = 30$, $\Delta = 0.5$ and different m parameter values.

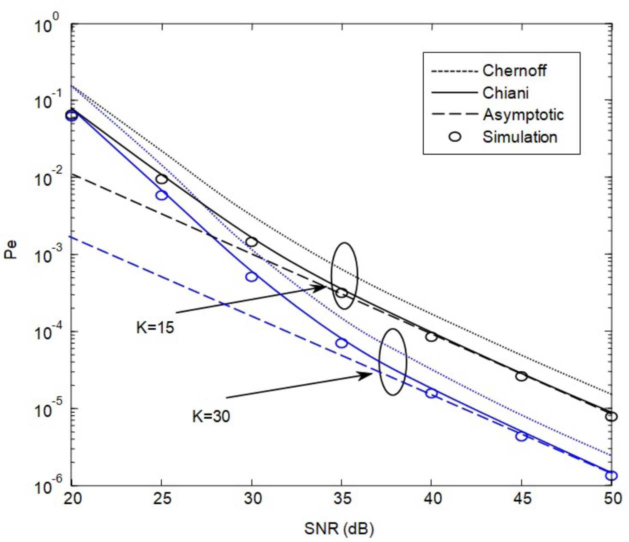

FIGURE 2. ASER performance of 8 × 4 RQAM with $m = 5$, $\Delta = 0.5$ and different K parameter values.

Then, an ASER expression for XQAM in the presence of FTR fading is obtained by inserting (29)-(34) into (26). To the best of the authors' knowledge, an ASER expression for XQAM over FTR fading has not been reported in the literature, yet.

IV. NUMERICAL RESULTS

We provide the numerical results for the proposed ASER expressions of RQAM and XQAM to show the effect of fading parameters of FTR distribution. It should be noted that infinite series are truncated after 40*th* terms to accurately calculate the derived expressions for all results in this paper. Analytical results of RQAM and XQAM are approved by the numerical solution of (5) and (26) by using Mathematica and Matlab softwares. Figs. 1 and 2 compare the Pe_{Chiani} and $Pe_{Chernoff}$ performances of 4 × 2 RQAM and 8 × 4

TABLE 1. Absolute relative difference between exact and approximate values of the chiani and chernoff approximations for ASER of 4 × 2 RQAM with $K = 30$, $\Delta = 0.5$, $m = 10$.

SNR (dB)	Approximation	R:Diff. (%)	Exact
30	Chiani: 4.420452 x10^{-6} Chernoff: 8.993893 x10^{-6}	14.5 133.0	3.859998 x10^{-6}
35	Chiani: 8.483311 x10^{-7} Chernoff: 1.568500 x10^{-6}	11.5 106.3	7.603103 x10^{-7}
40	Chiani: 2.253308 x10^{-7} Chernoff: 4.005226 x10^{-7}	10.2 95.9	2.044034 x10^{-7}

TABLE 2. Absolute relative difference between exact and approximate values of the chiani and chernoff approximations for ASER of 8 × 4 RQAM with $K = 15$, $\Delta = 0.5$, $m = 5$.

SNR (dB)	Approximation	R:Diff. (%)	Exact
40	Chiani: 0.000094 *Chernoff*: 0.000164	10.58 92.94	0.000085
45	Chiani: 0.000028 Chernoff: 0.000048	12.0 92.0	0.000025
50	Chiani: 8.831291x10^{-6} Chernoff: 0.000015	10.08 86.97	8.022451x10^{-6}

RQAM over FTR fading channels for different configurations of parameters.

While Fig. 1 shows the effect of the m parameter for 4 × 2 RQAM with $K = 30$, $\Delta = 0.5$, the impact of K parameter for 8 × 4 RQAM with $\Delta = 0.5$, $m = 5$ is presented in Fig. 2. In Fig 1, it can be observed that as value of the m parameter increases, the performance of 4 × 2 RQAM system over mmWave FTR fading channels improves. For example, an ASER of 10^{-4} occurs at $\overline{\gamma} \approx 30$ dB when $m = 5$ and the same ASER value occurs at $\overline{\gamma} \approx 23$ dB when $m = 10$. On the other hand in Fig 2, an ASER level of 10^{-3} takes place at $\overline{\gamma} \approx 28$ dB when $K = 30$, the same ASER result with $K = 15$ occurs at $\overline{\gamma} \approx 33$ dB. It can be concluded that increasing value of K provides performance improvement of 8 × 4 RQAM system over mmWave FTR fading channels. Furthermore, the asymptotic behaviors of both 4 × 2 RQAM and 8 × 4 RQAM are given in Figs 1 and 2. It should be emphasized that the asymptotic curves are close to analytical curves and simulations at high SNR regime. Besides, when the 40 terms are used for the infinite series, Table I tabulates the absolute relative difference values for ASER of 4 × 2 RQAM with $K = 30$, $\Delta = 0.5$, $m = 10$ over mmWave FTR fading channels.

We can see from these results that the simulations of the RQAM over FTR fading become very tight with theoretical results for all SNR values. From the Fig 1, one can see that the best performance is obtained with $m = 10$. It is observed that Pe_{Chiani} results are closer than the $Pe_{Chernoff}$ results to the analytical findings for all fading parameter configurations since the Chiani approximation is tighter than the Chernoff approximation. The Chiani approximation for Gaussian Q-function includes two exponential terms, so it ensures

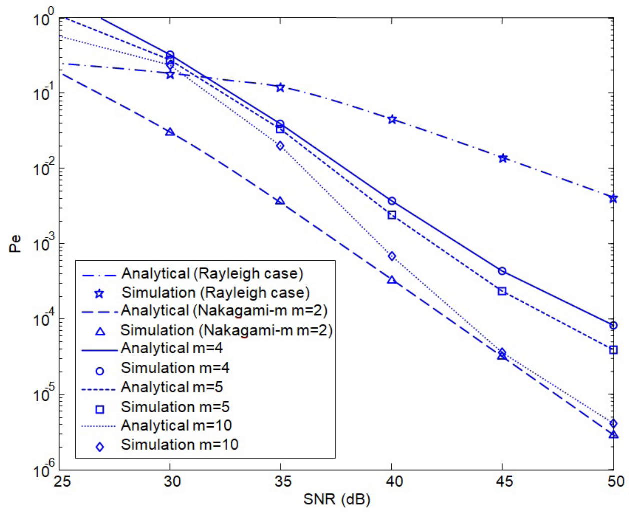

FIGURE 3. ASER performance of 32-XQAM over FTR fading channels.

preferable agreement with the simulations when compared to the Chernoff approximation which contains one exponential term for Gaussian Q-function. For this reason, the ASER results of RQAM over mmWave FTR channels obtained from the Chiani approximation indicate good agreement to the simulations. This can be viewed as the reason for the deviation of the results obtained by two bounds.

The absolute relative difference percentage for ASER of 8×4 RQAM with $K = 15$, $\Delta = 0.5$, $m = 5$ over mmWave FTR fading channels is given in Table II by using the first 40 terms for the infinite series in the approximate ASER expressions. In addition, Table III presents the results of evaluating the ASER expressions in (14) and (23) at a certain upper limit namely J. The table demonstrates the decimal places that have not been affected with adding more terms to the summations, in bold. From table III, it is clear that the first 40 terms for the ASER calculation of RQAM is quite sufficient.

In Fig. 3, the ASER performance of 32-XQAM under FTR fading conditions is illustrated when $K = 30$, $\Delta = 0.5$, $m = 4$, 5 and 10. The ASER performance of XQAM scheme with $m = 10$ outperforms the performance of XQAM with $m = 4, 5$ as expected since the higher m parameter values correspond to good fading conditions in FTR channels. In this figure, the results of the special cases are provided for mmWave FTR fading channels as Nakagami-m case ($K \rightarrow \infty$, $\Delta = 0$, $m = m$) and Rayleigh case ($K \rightarrow \infty$, $\Delta = 0$, $m = 1$) are included. The case of $\Delta = 0$, $K \rightarrow \infty$, $m = 1$ represents NLOS environments as the channel model turns into Rayleigh fading. In order to reflect the LOS effects, the fading parameters should be set as $\Delta = 0$, $K = K$, $m \rightarrow \infty$ which corresponds to the case of Rician fading. It should be noted that the analytical results are very close to the exact simulations for 32-XQAM. By these means, the accuracy of analytical work proposed in this study is demonstrated. In Table IV, the results of evaluating the ASER expression of XQAM by inserting (29)-(34) into (26)

TABLE 3. Values of ASER with cherfnoff (14) and chiani (23) approximations for different levels of truncation ($\overline{\gamma} = 35$ dB, $K = 15$, $\Delta = 0.5$, $m = 5$).

J	Chernoff Approx. eq. (14)	Chiani Approx. eq. (23)
1	**0.00001**682165338591817	**9.**417798128578183x10^{-6}
5	**0.00001**730452166674863	**9.**604537283503918x10^{-6}
10	**0.000017304**54603396355	**9.6045**43115246886x10^{-6}
20	**0.00001730454603**336928	**9.6045431152**71153x10^{-6}
30	**0.0000173045460339**8962	**9.604543115251713**x10^{-6}
40	**0.00001730454603398962**	**9.604543115251713**x10^{-6}

TABLE 4. Values of ASER FOR 32-XQAM with $H = 100$ and $R = 40$ for different levels of truncation ($\overline{\gamma} = 45$ dB, $K = 30$, $\Delta = 0.5$, $m = 4$).

J	Analytical expression eq. (26)
1	**0.000**28722918305668550
5	**0.000**44065811379191347
10	**0.00044**110649292435000
20	**0.000441106**50224934306
30	**0.0004411065022**3034946
40	**0.00044110650223034946**

at upper limits J, H and R are illustrated. It is seen that 40 terms for the ASER computation of XQAM are enough to get a given accuracy in this paper.

V. CONCLUSION

In this study, we have presented the ASER performance of RQAM and XQAM signaling schemes over millimeter wave FTR fading channels. New and novel expressions are derived and evaluated for various configurations of channel parameters. An exact ASER expression of RQAM over millimeter wave FTR fading channels is obtained. In addition to this, two upper bound ASER expressions are proposed for RQAM scheme based on two different approximations of Gaussian Q-function for comparison purpose. Then, an exact ASER expression is obtained for the ASER of XQAM technique in terms of infinite series representation. Furthermore, the analytical results are validated by exact simulations which show the accuracy of proposed analysis in this paper.

REFERENCES

[1] N. Kumar, P. K. Singya, and V. Bhatia, "ASER analysis of hexagonal and rectangular QAM schemes in multiple-relay networks," *IEEE Trans. Veh. Technol.*, vol. 67, no. 2, pp. 1815–1819, Feb. 2018.
[2] M. Nakazawa, M. Yoshida, K. Kasai, and J. Hongou, "20 msymbol/s, 64 and 128 QAM coherent optical transmission over 525 km using heterodyne detection with frequency-stabilised laser," *IET Electron. Lett.*, vol. 42, no. 12, pp. 710–712, Jun. 2006.
[3] L. Hanzo, W. Webb, and T. Keller, *Single- and Multi-Carrier Quadrature Amplitude Modulation*. New York, NY, USA: Wiley, 2000.
[4] G. L. Stüber, *Principles of Mobile Communication*, 2nd ed. Norwell, MA, USA: Kluwer, 2003.
[5] J. G. Proakis, *Digital Communications*, 4th ed. New York, NY, USA: McGraw-Hill, 2001.
[6] D. P. Agrawal and Q.-A. Zeng, *Introduction to Wireless and Mobile Systems*, 3nd ed. Hoboken, NJ, USA: Wiley, 2011.
[7] T. S. Rappaport, *Wireless Communication*, 2nd ed. Chennai, India: Pearson, 2011.

[8] J. G. Smith, "Odd-bit quadrature amplitude-shift keying," *IEEE Trans. Commun.*, vol. 23, no. 3, pp. 385–389, Mar. 1975.
[9] *Asymmetric Digital Subscriber Line (ADSL) Transceivers*, ITU-T Standard G.992.1, Jun. 1999.
[10] *Very High Speed Digital Subscriber Line Transceiver*s, ITU-T Standard G.993.1, Jun. 2004.
[11] *Digital Video Broadcasting (DVB); Framing Structure, Channel Coding and Modulation for Cable Systems*, ETSI Standard EN 300 429, Apr. 1998.
[12] D. Dixit and P. R. Sahu, "Performance of QAM signaling over TWDP fading channels," *IEEE Trans. Wireless Commun.*, vol. 12, no. 4, pp. 1794–1799, Apr. 2013.
[13] H. Yu, G. Wei, F. Ji, and X. Zhang, "On the error probability of cross-QAM with MRC reception over generalized η-μ fading channels," *IEEE Trans. Veh. Technol.*, vol. 60, no. 6, pp. 2631–2643, Jul. 2011.
[14] N. Kumar and V. Bhatia, "Exact ASER analysis of rectangular QAM in two-way relaying networks over Nakagami-*m* fading channels," *IEEE Wireless Commun. Lett.*, vol. 5, no. 5, pp. 548–551, Oct. 2016.
[15] D. Dixit and P. R. Sahu, "Performance analysis of rectangular QAM with SC receiver over Nakagami- *m* fading channels," *IEEE Commun. Lett.*, vol. 18, no. 7, pp. 1262–1265, Jul. 2014.
[16] P. K. Singya, N. Kumar, and V. Bhatia, "Impact of imperfect CSI on ASER of hexagonal and rectangular QAM for AF relaying network," *IEEE Commun. Lett.*, vol. 22, no. 2, pp. 428–431, Feb. 2018.
[17] N. Kumar and V. Bhatia, "Performance evaluation of QAM schemes for multiple AF relay network under Rayleigh fading channels," *Wireless Pers. Commun.*, vol. 99, no. 1, pp. 567–580, Mar. 2018.
[18] W. M. Jang, "A simple performance approximation of general-order rectangular QAM with MRC in Nakagami- *m* fading channels," *IEEE Trans. Veh. Technol.*, vol. 62, no. 7, pp. 3457–3463, Sep. 2013.
[19] P. K. Singya, N. Kumar, V. Bhatia, and F. A. Khan, "Performance analysis of OFDM based 3-hop AF relaying network over mixed Rician/Rayleigh fading channels," *AEU-Int. J. Electron. Commun.*, vol. 93, pp. 337–347, Sep. 2018.
[20] M. W. Kamdar and H. Xu, "Performance analysis of cross QAM with MRC over dual correlated Nakagami-m, -n, and -q channels," *Wireless Pers. Commun.*, vol. 84, no. 4, pp. 3015–3030, Oct. 2015.
[21] Q. U. Khan, S. Viqar, and S. A. Sheikh, "Two novel blind equalization algorithms for rectangular quadrature amplitude modulation constellations," *IEEE Access*, vol. 4, pp. 9512–9519, 2016.
[22] M. Bilim, "QAM signaling over $k-\mu$ shadowed fading channels," *Phys. Commun.*, vol. 34, pp. 261–271, Jun. 2019.
[23] D. Singh and H. D. Joshi, "Error probability analysis of STBC-OFDM systems with CFO and imperfect CSI over generalized fading channels," *Int. J. Electron. Commun.*, vol. 98, pp. 156–163, Jan. 2018.
[24] D. Singh and H. D. Joshi, "Error probability analysis of STBC-OFDM systems with CFO and imperfect CSI over generalized fading channels," *AEU-Int. J. Electron. Commun.*, vol. 98, pp. 156–163, Jan. 2019.
[25] J. M. Romero-Jerez, F. J. Lopez-Martinez, J. F. Paris, and A. Goldsmith, "The fluctuating two-ray fading model for mmWave communications," in *Proc. IEEE Globecom Workshops (GC Wkshps)*, Dec. 2016, pp. 1–6.
[26] J. M. Romero-Jerez, F. J. Lopez-Martinez, J. F. Paris, and A. J. Goldsmith, "The fluctuating two-ray fading model: Statistical characterization and performance analysis," *IEEE Trans. Commun.*, vol. 16, no. 7, pp. 4420–4432, Jul. 2017.
[27] S. Sun, H. Yan, G. R. MacCartney, and T. S. Rappaport, "Millimeter wave small-scale spatial statistics in an urban microcell scenario," in *Proc. IEEE Int. Conf. Commun.*, May 2017, pp. 1–7.
[28] J. Zhang, W. Zeng, X. Li, Q. Sun, and K. P. Peppas, "New results on the fluctuating two-ray model with arbitrary fading parameters and its applications," *IEEE Trans. Veh. Technol.*, vol. 67, no. 3, pp. 2766–2770, Mar. 2018.
[29] W. Zeng, J. Zhang, S. Chen, K. P. Peppas, and B. Ai, "Physical layer security over fluctuating two-ray fading channels," *IEEE Trans. Veh. Technol.*, vol. 67, no. 9, pp. 8949–8953, Sep. 2018.
[30] H. Zhao, Z. Liu, and M.-S. Alouini, "Different power adaption methods on fluctuating two-ray fading channels," *IEEE Wireless Commun. Lett.*, vol. 8, no. 2, pp. 592–595, Apr. 2019.
[31] I. S. Gradshteyn and I. M. Ryzhik, *Table of Integrals, Series and Products*, 6th ed. San Diego, CA, USA: Academic, 2000.
[32] N. C. Beaulieu, "A useful integral for wireless communication theory and its application to rectangular signaling constellation error rates," *IEEE Trans. Commun.*, vol. 54, no. 5, pp. 802–805, May 2006.
[33] A. P. Prudnikov, Y. A. Brychkov, and O. I. Marichev, *Integrals and Series: More Special Functions*, vol. 3. New York, NY, USA: Gordon & Breach, 1990.
[34] Accessed: Jun. 10, 2019. [Online]. Available: http://functions.wolfram.com
[35] J. M. Wozencraft and I. M. Jacobs, *Principles of Communication Engineering*. Hoboken, NJ, USA: Wiley, 1965, p. 83.
[36] M. Chiani, D. Dardari, and M. K. Simon, "New exponential bounds and approximations for the computation of error probability in fading channels," *IEEE Trans. Wireless Commun.*, vol. 2, no. 4, pp. 840–845, Jul. 2003.
[37] M. K. Simon and M.-S. Alouini, *Digital Communication Over Fading Channels*, 2nd ed. New York, NY, USA: Wiley, 2005.
[38] M. Abramowitz and I. A. Stegun, *Handbook of Mathematical Functions with Formulas, Graphs and Mathematical Tables*, 9th ed. New York, NY, USA: Dover, 1972.

MEHMET BILIM was born in Gaziantep, Turkey. He received the B.Sc., M.Sc., and Ph.D. degrees in electrical and electronics engineering from Erciyes University, Turkey, in 2010, 2012, and 2018, respectively, where he was a Research Assistant with the Department of Electrical and Electronics Engineering, from 2011 to 2018. He is currently an Assistant Professor with the Department of Electrical and Electronics Engineering, Nuh Naci Yazgan University. He is also the author of more than 30 papers in major conferences and journals. He teaches courses in wireless communications, and his current research interests include spread spectrum communications, multiuser communications, multiple access techniques, wireless networks, millimeter wave communications, digital communications, fading channels, cooperative diversity, and applications of neural networks to communication systems. He was a recipient of the Ph.D. Research Fellowships from the Scientific and Technological Research Council of Turkey (TUBITAK). He was a recipient of the Best Presenter Award from the ICAT International Conference 2016. He is a Reviewer of the IEEE, Elsevier, Wiley, Springer, and IET journals.

NURI KAPUCU received the B.Sc., M.Sc., and Ph.D. degrees in electrical and electronics engineering from Erciyes University, Turkey, in 2010, 2012, and 2017, respectively, where he was a Research Assistant with the Department of Electrical and Electronics Engineering, from 2011 to 2018. He is currently an Assistant Professor with the Department of Electrical and Electronics Engineering, Hitit University. His current research interests include performance analysis over fading channels, cooperative communications, two-way relaying, and multiple access techniques.